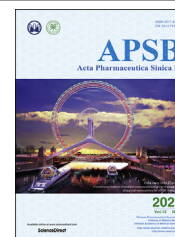




Chinese Pharmaceutical Association
Institute of Materia Medica, Chinese Academy of Medical Sciences

Acta Pharmaceutica Sinica B

www.elsevier.com/locate/apsb
www.sciencedirect.com



ORIGINAL ARTICLE

Aristolochic acids exposure was not the main cause of liver tumorigenesis in adulthood



Shuzhen Chen^{a,b,†}, Yaping Dong^{a,b,d,e,†}, Xinming Qi^{c,†}, Qiqi Cao^{a,b,†},
Tao Luo^{f,g}, Zhaofang Bai^h, Huisi He^{a,b}, Zhecai Fan^{a,b}, Lingyan Xu^{a,b},
Guozhen Xing^c, Chunyu Wang^h, Zhichao Jinⁱ, Zhixuan Li^{a,b},
Lei Chen^{a,b}, Yishan Zhong^a, Jiao Wang^{f,g}, Jia Ge^{f,g}, Xiaohe Xiao^h,
Xiuwu Bian^{f,g}, Wen Wen^{a,b,*}, Jin Ren^{c,*}, Hongyang Wang^{a,b,d,e,*}

^aNational Center for Liver Cancer, Second Military Medical University, Shanghai 200438, China

^bInternational Cooperation Laboratory on Signal Transduction, Eastern Hepatobiliary Surgery Hospital, Second Military Medical University, Shanghai 200438, China

^cCenter for Drug Safety Evaluation and Research, State Key Laboratory of Drug Research, Shanghai Institute of Materia Medica, Chinese Academy of Sciences, Shanghai 201203, China

^dFudan University Shanghai Cancer Center, Shanghai 200032, China

^eThe Graduate School of Fujian Medical University, Fuzhou 350122, China

^fInstitute of Pathology, Southwest Hospital, Third Military Medical University (Army Medical University), Chongqing 400038, China

^gKey Laboratory of Tumor Immunopathology, Ministry of Education of China, Chongqing 400038, China

^hChina Military Institute of Chinese Materia, Fifth Medical Center of Chinese PLA General Hospital, Beijing 100039, China

ⁱDepartment of Health Statistics, Faculty of Medical Service, Second Military Medical University, Shanghai 200438, China

Received 18 September 2021; received in revised form 25 October 2021; accepted 27 October 2021

Abbreviations: AAs, aristolochic acids; AAI, Aristolochic acid I; AL, aristolactam; dA-ALI, 7-deoxyadenosin-^N₆-yl aristolactam I; COSMIC, Catalogue of Somatic Mutations in Cancer; HBV, hepatitis B virus; HCC, hepatocellular carcinoma; EHBH, Eastern Hepatobiliary Surgery Hospital; CHERRY, Chinese Electronic Health Records Research; FFPE, formalin-fixed paraffin-embedded; SNV, somatic single nucleotide variant; AFP, alpha fetoprotein; MVI, microvessel invasion; WGS, whole genome sequencing; TCGA, The Cancer Genome Atlas; ALT, alanine aminotransferase; AST, aspartate aminotransferase; CRE, creatinine; DEN, *N*-nitrosodiethylamine; WT, wild type.

*Corresponding authors. Tel.: +86 21 81875361, fax: +86 21 65566851 (Hongyang Wang); Tel.: +86 21 81875363; fax: +86 21 65566851 (Wen Wen)

E-mail addresses: hywangk@vip.sina.com (Hongyang Wang), jren@cdser.simm.ac.cn (Jin Ren), wenwen_smmu@163.com (Wen Wen).

[†]These authors made equal contributions to this work.

Peer review under responsibility of Chinese Pharmaceutical Association and Institute of Materia Medica, Chinese Academy of Medical Sciences

<https://doi.org/10.1016/j.apsb.2021.11.011>

2211-3835 © 2022 Chinese Pharmaceutical Association and Institute of Materia Medica, Chinese Academy of Medical Sciences. Production and hosting by Elsevier B.V. This is an open access article under the CC BY-NC-ND license (<http://creativecommons.org/licenses/by-nc-nd/4.0/>).

KEY WORDS

Aristolochic acids (AAs);
 Mutational signature;
 AA–DNA adduct;
 Hepatocellular carcinoma
 (HCC);
 Liver tumorigenesis;
 Hepatitis B virus (HBV);
 Risk factors;
 Tumor prevention

Abstract Aristolochic acids (AAs) have long been considered as a potent carcinogen due to its nephrotoxicity. Aristolochic acid I (AAI) reacts with DNA to form covalent aristolactam (AL)–DNA adducts, leading to subsequent A to T transversion mutation, commonly referred as AA mutational signature. Previous research inferred that AAs were widely implicated in liver cancer throughout Asia. In this study, we explored whether AAs exposure was the main cause of liver cancer in the context of HBV infection in mainland China. Totally 1256 liver cancer samples were randomly retrieved from 3 medical centers and a refined bioanalytical method was used to detect AAI–DNA adducts. 5.10% of these samples could be identified as AAI positive exposure. Whole genome sequencing suggested 8.41% of 107 liver cancer patients exhibited the dominant AA mutational signature, indicating a relatively low overall AAI exposure rate. In animal models, long-term administration of AAI barely increased liver tumorigenesis in adult mice, opposite from its tumor-inducing role when subjected to infant mice. Furthermore, AAI induced dose-dependent accumulation of AA–DNA adduct in target organs in adult mice, with the most detected in kidney instead of liver. Taken together, our data indicate that AA exposure was not the major threat of liver cancer in adulthood.

© 2022 Chinese Pharmaceutical Association and Institute of Materia Medica, Chinese Academy of Medical Sciences. Production and hosting by Elsevier B.V. This is an open access article under the CC BY-NC-ND license (<http://creativecommons.org/licenses/by-nc-nd/4.0/>).

1. Introduction

Aristolochic acids (AAs) are natural compounds that are widely present in genera of *Aristolochia*, *Bragantia* and *Asarum*¹, commonly used in herbal medicine and traditional Chinese medicine. Due to its well-defined nephrotoxicity, herbal remedies containing plant species of the genus *Aristolochia* were listed as Group 1 carcinogen by the International Agency for Research on Cancer. As early as the 1990s, AA-containing herbs were found to cause kidney failure in women taken pills for weight loss at Belgian^{2,3}. AA was also responsible for AA-associated urothelial cancer^{4,5} and bladder cancer⁶, etc. Therefore, the use of herbs with AAs was prohibited or limited worldwide. As a country with large consumption of herbs in traditional Chinese medicine, AA-containing plants have been banned in Taiwan (China) since 2003 and in Hong Kong (China) since 2004. Some AA-containing herbs were also banned in mainland China. According to China Food and Drug Administration, there were still 43 *Aristolochia*-containing drugs and 24 possible AAs-containing crude drugs in circulation up to 2017.

Aristolochic acid I (AAI) is the well-defined carcinogenic component of *Aristolochia* species both in human and rodents^{7,8}. AAI reacts with DNA to form covalent aristolactam (AL)–DNA adducts, that is, 7-deoxyguanosin-*N*²-yl aristolactam I and 7-deoxyadenosin-*N*⁶-yl aristolactam I (dA-ALI)^{9,10}. dA-ALI is by far the most abundant form of AA–DNA adduct found in human kidney¹¹. AA–DNA adducts could still be detected many years after AA exposure was ceased, showing remarkable persistence in human tissues^{12,13}. dA-ALI were responsible for the subsequent A to T transversion mutation in patients with aristolochic acid nephropathy in Taiwan area of China⁵ and AA-caused upper urinary tract urothelial cell carcinoma¹⁴. Therefore, dA-AL is often considered as biomarkers of AA exposure, and A to T transversion (Catalogue of Somatic Mutations in Cancer [COSMIC] signature 22) is commonly referred as AA mutational signature.

Liver cancer is one of the most heterogeneous malignancies worldwide with multiple risk factors, and the most well-known is hepatitis B virus (HBV) infection¹⁵. Hepatocellular carcinoma (HCC) accounts for about 85% of all primary liver malignancies¹⁵. In 2012, a research has reported that 4 out of 10 HBV-related HCC

patients from China showed significant A to T transversion¹⁶. It was not until 2017 that AA was under spotlight for its association with liver cancer in Taiwan area of China and throughout Asia. This study sequenced the whole exomes of 98 HCCs from Taiwan area and revealed that 78% showed the mutational signature of AA exposure¹⁷. Another study analyzed the mutation profile of 159 HBV-related HCC patients in China and identified AA signature mutation in 56 tumors¹⁸. These studies implicated the potential association of AA exposure with HCC mainly based on data analysis. However, direct evidence linking AA consumption to HCC in adulthood is absent. Besides, considering the fact that most of HCC patients in China are related to HBV infection, whether AA exposure could outweigh the power of HBV as the main risk factor of HCC needs to be carefully investigated.

In this study, we aimed to explore if there is a causal link between AA exposure and HCC development *via* cohort study and mouse models. Significantly, we detected 1256 randomly selected HCC patient samples from 3 medical centers, of which 64 were identified as dA-ALI positive, indicating a low AA exposure rate. Meanwhile, mutational spectra of 107 HCC patients did not show a dominant AA mutational signature. From a retrospective study, HBV infection other than AA exposure increased the risk of HCC in a cohort of 9977 patients. Meanwhile, AAI did not increase liver tumorigenesis when administered to adult mice. We also explored whether AA could cooperate with HBV infection to accelerate HCC in transgenic mice. dA-ALI and AA mutational signatures were also detected in these samples.

2. Methods and materials**2.1. Patients and samples**

One hundred and seven patients who underwent liver resection between January 2018 and October 2019 at Eastern Hepatobiliary Surgery Hospital (EHBH, Shanghai, China) for clinical pathologically confirmed HCC were included for whole genome sequencing analysis. Matched pairs of fresh primary HCC samples and adjacent normal liver tissue were obtained. This investigation was approved by Eastern Hepatobiliary Surgery Hospital Ethics

Committee. Informed consent was obtained from patients prior to surgery.

For dA-ALI detection, we collected 1256 formalin-fixed, paraffin-embedded (FFPE) tissues of HCC patients from 3 medical centers in mainland China. Cohort 1 included 925 samples from Eastern Hepatobiliary Surgery Hospital in Shanghai, China. Cohort 2, containing 277 samples, was obtained from Southwest Hospital located in Chongqing, China. Cohort 3 contained samples of 54 patients from the Fifth Medical Center of Chinese People's Liberation Army General Hospital, located in Beijing, China. These samples with the diagnosis of HCC within five years were randomly selected according to their availability. This study was approved by Ethics Committee of EHBH, Southwest Hospital and the Fifth Medical Center of Chinese People's Liberation Army General Hospital, respectively. Informed consent was obtained prior to surgery from each patient.

2.2. Animal experiments

C57BL/6 and BALB/c mice were obtained from the China Academy of Science (Shanghai, China). C57BL/6-TgHBV mice were purchased from Shanghai Model Organisms Center, Inc. (Shanghai, China). High-level expression HBV transgenic BALB/c mice were obtained from Transgenic Engineering Research Laboratory, Infectious Disease Center of People's Liberation Army (Guangzhou, China). All animals were maintained at an animal facility under specific pathogen-free conditions and received humane care according to the criteria outlined in the "Guide for the Care and Use of Laboratory Animals" and the animal experiments protocols approved by the Institutional Animal Care and Use Committee of the Second Military Medical University, Shanghai, China.

For C57BL/6, C57BL/6-TgHBV, BALB/c and BALB/c-TgHBV adult mice model, animals were given indicated doses of AAI (Sigma, St. Louis, MO, USA) or the control (1% NaHCO₃, Sinopharm Chemical Reagent Co., Shanghai, China) by gavage at the age of 8 weeks. For mice with AAI administration alone, AAI was given consecutively every other week. The total duration of AAI administration was 8 months. For C57BL/6 and C57BL/6-TgHBV mice with the combined treatment of CCl₄ (Sinopharm Chemical Reagent Co., Shanghai, China) and AAI, CCl₄ (0.5 mL/kg) was injected intraperitoneally once a week for a duration of 8 months. AAI was administered as described above. For BALB/c and BALB/c-TgHBV mice with the combined treatment of CCl₄ and AAI, CCl₄ (0.5 mL/kg) was injected intraperitoneally once a week, and AAI was administered at the same frequency as described above for a total duration of 2 months. For each group with AAI, more than 20 mice were used to observe the long-term effect of AAI on different organs such as the forestomach, liver and kidney.

For the infant mouse model, a single dose of AAI (10 or 20 mg/kg) was given intraperitoneally 14 days after birth. Chemical carcinogen *N*-nitrosodiethylamine (DEN, 20 mg/kg, Sigma, St. Louis, MO, USA) was administered as a positive control. For each group, at least six mice were sacrificed at each time point to observe the effect of AAI or DEN. For mice with CCl₄ combined treatment to accelerate tumorigenesis, CCl₄ (0.5 mL/kg) was administered intraperitoneally 2 weeks after the single shot of DEN or AAI per week for 18 weeks. In AAI supplemented model, AAI (3.0 mg/kg) was given consecutively every other week started one week after the first injection of CCl₄. For

each group, more than 15 mice were used to observe the long-term effect of AAI on liver tumorigenesis.

2.3. Analysis of dA-ALI

2.3.1. dA-ALI synthesis

7-Deoxyadenosin-*N*⁶-yl aristolactam I (dA-ALI) was synthesized based on Suzuki–Miyaura coupling reaction. The final coupling step that produced the adduct and ¹H NMR spectrum was described in the Ref. 19. The productive rate of dA-ALI synthesis was 0.24%, and the purity by HPLC was 97.8%.

2.3.2. Deparaffinization, rehydration, and DNA isolation from FFPE tissues

The HCC samples were cut out of the block, and two tissue-sections of 10 μm-thickness were transferred to a 1.5 mL Eppendorf tube and submerged with xylene (1.0 mL), washed with xylene for 3 times, and then washed with descending ethanol/water, followed by final rehydration with water. DNA was isolated by *Quick*-DNA FFPE MiniPrep Kit (Zymo Research, CA, USA). The protocol followed the manufacturer's instructions with minor modifications. Due to the variation of tissue size and extracellular matrix content among FFPE samples, the DNA concentrations of many samples were lower than 50 ng/μL, which Nanodrop could not accurately measure. Therefore, we used Quant-iT PicoGreen dsDNA Assay Kit (ThermoFisher, Waltham, MA, USA) to detect the concentration of DNA recovered from FFPE tissues.

2.3.3. DNA digestion and protein precipitation

48 μL purified DNA was used for the DNA digestion. 1.5 μL DNase I (2542 U/mL in 0.15 mol/L NaCl; 254.2 U/mg DNA; Sigma) was added, and incubated at 37 °C for 1.5 h. Next, 1 μL nuclease P1 (100 U/mL in 1 mmol/L ZnCl₂; 4 U/mg DNA; Sigma) was added, and incubated at 37 °C for 3 h. 1.5 μL alkaline phosphatase (24 U/mL in 1 mmol/L MgCl₂; 2 U/mg DNA; Sigma) and 8 μL phosphodiesterase I (1.7 U/mL in 110 mmol/L Tris-HCl at pH 8.9 containing 110 mmol/L NaCl, 15 mmol/L MgCl₂, and 50% glycerol; 0.0714 U/mg DNA; Sigma) were added, and incubated at 37 °C for 18 h. After incubation, 60 μL internal standard (IS) solution was added into 60 μL above mixture for protein precipitation and centrifuged at 12,000 rpm for 5 min. 110 μL supernatant was transferred to 96-well plate for LC–MS/MS analysis.

2.3.4. Qualitative and quantitative analysis of dA-ALI

dA-ALI was analyzed with an ultra-performance liquid chromatography (UPLC) system (LC-30, SHIMAZU, Tokyo, Japan) connected to a Triple Quad 6500+ System (UPLC–MS/MS, AB Sciex LLC, MA, USA) with electrospray ionization (ESI). The separation was carried out on an ACE C18 column (50 mm × 2.1 mm, 5 μm) maintained at 40 °C. A gradient program was conducted using an aqueous mobile phase A of 0.2% acetic acid in water and an organic mobile phase B of acetonitrile. Flow rate was set at 0.5 mL/min through each injection. The injection volume was 15 μL and the retention time of the dA-AAI (Analyte) and AAI (IS) were 1.19 min and 1.42 min, respectively. The gradient program used followed previous report¹⁹. Detection of the ion pairs was performed by multiple reaction monitoring (MRM) mode fitted with electrospray ionization (ESI) probe and operated in the positive ion mode. The MRM ion pairs for dA-ALI were 543.2/427.1 and 543.2/395.2. The optimized conditions were as follows: Curtain Gas, 40 psi; Collision Gas, 10 psi; IonSpray Voltage, 5000 V; Temperature, 550 V; Ion Source

Gas 1, 50 psi; Ion Source Gas 2, 50 psi; Entrance Potential, 10 V; Collision Cell Exit Potential, 15 V. The MRM transitions and the related optimized declustering potential (DP), collision energy (CE) for dA-AAI and IS are shown in Table 1. Data were acquired and analyzed by Analyst 1.6.3. For the qualification of dA-ALI, the following criteria were used: signal to noise ratio should be ≥ 3 and relative abundance variation between two ion pairs should be $\leq 50\%$ (when one of production content is $\leq 10\%$ that of another product ion in total ion current). For the quantification of dA-ALI, a limit of detection at 5 pg/mL was selected and validated its accuracy, stability and precision¹⁹.

2.4. Statistical analysis

Data analysis was performed using the SPSS software (version 22) and R (v.3.6.2). Values were presented as mean \pm standard deviation (SD). Competing risk analysis was used for mice survival analysis. In the community population of HCC and non-HCC, associations between risk variables and HCC were explored *via* logistic regression. Student's *t*-test was applied when normality and homogeneity of variance assumptions were satisfied otherwise the Chi-square test and Mann Whitney test were used. All tests of *P* values were two-sided. Values of *P* less than 0.05 were considered statistically significant.

Additional details are available in Supporting Information.

3. Results

3.1. dA-ALI positive rate was low in HCCs from multi-centered samples in mainland China

AA–DNA adduct was considered as a marker of AA exposure for AA nephropathy-associated cancer and upper urothelial cancer²⁰. In this study, we used a refined method to quantify dA-ALI in a total of 1256 HCC patients from 3 medical centers. These samples covered 31 provinces and municipalities in mainland China (Fig. 1A). Cohort 1 was obtained from a hospital located in Shanghai, with a total of 925 patients. Cohort 2 ($n = 277$) was from a hospital located in the southwest China, where herbal medicine might be more commonly used by minority ethnic groups reside in this area. Cohort 3 ($n = 54$) was from Beijing, located in the North of China. The threshold for positive dA-ALI detection was identified as 5 pg/mL and samples with peaks were considered as dA-ALI detectable. The accuracy, stability and precision of the method developed were validated¹⁹.

Among the 3 cohorts, cohort 1 has a dA-ALI positivity of 5.73%, with 53 out of 925 patients above the threshold of 5 pg/mL. Seven hundred twenty-one samples (77.95%) were below the limit of detection, with no peak detected. The positive rates of dA-ALI in cohort 2 and cohort 3 were 3.25% and 3.70%, respectively, even lower than cohort 1. Taken the 3 cohorts together, a total of 64 patients out of 1256 (5.10%) were identified

as dA-ALI positive and another 13.93% (175/1256) had detectable peaks (Fig. 1B). From the above data, dA-ALI was only detected in a small proportion of HCC patients, indicating a relatively low AA exposure rate. The distribution of dA-ALI abundance in positive patients was presented as pg/mL and dA-ALI per 10⁶ nucleotides relatively in Fig. 1C. The clinicopathological features between dA-ALI positive patients and negative patients in cohort 1 and cohort 2 revealed no significant preference of dA-ALI distribution to variables, such as age, gender, HBV infection or tumor size (Supporting Information Tables S1 and S2).

Next, we investigated if AA correlated with HCC development in a retrospective cohort study. The Chinese Electronic Health Records Research (CHERRY) was designed to establish a longitudinal population-based ambispective cohort study for tracing the complete lifetime healthcare journal for one million adults in Yinzhou, an eastern coastal area of China²¹. In this study, we extracted a sub-cohort ($n = 9977$) with the history of traditional Chinese medicine consumption from the CHERRY study cohort, including 127 HCC patients and 9850 non-HCC patients (Supporting Information Fig. S1A). Four variables were extracted from the database, including three well-defined risk factors of HCC (gender, age, HBV infection) and AAs-containing drug exposure history (Fig. S1B). 47 out of 127 (37.01%) patients in HCC group had medical records of AAs-containing drug consumption. While in control group, the AA exposure rate was nearly 50%. Logistic regression analysis showed that gender, age and HBV infection were significant risk factors of HCC development, especially HBV infection with an OR of 106.119 ($P < 0.0001$). However, the OR of AA exposure to HCC was 0.683 ($P = 0.082$), indicating that AAs exposure didn't increase the risk of HCC in this sub-cohort (Fig. S1B). Therefore, these data suggest that AAs exposure might not be the main contributor of HCC in our cohorts.

3.2. Low AA mutational signature in HCCs from EHBH cohort

Since AA–DNA adduct could cause characteristic A to T transversion in the genome, we next investigated the proportion of AA mutational signature in HCC patients. One hundred seven patients were randomly selected from cohort 1, comprised of dA-ALI detectable samples ($n = 23$) and undetectable samples ($n = 84$). Clinical characteristics of HCC patients are presented in Supporting Information Table S3. We sequenced the whole genome of tumor tissues and matched nonmalignant tissues, with a mean of 89.89% targeted tumor bases $\geq 30 \times$ coverage. A total of 18,165 somatic single nucleotide variants (SNV) across the HCCs were detected (median, 146 SNVs per tumor). A total of 7942 short insertions or deletions were identified. Driver gene analysis with MutSigCV identified significantly mutated genes. Among them, *TP53*, *CTNNB1* and *AXIN1* were the most commonly mutated genes reported in HCC²² (Supporting Information Fig. S2A). We also detected the mutation of driver genes identified in the Cancer Genome Atlas (TCGA), of which *TP53* mutation occurred in 44% of tumors (Fig. S2A).

The mutational spectra of 107 patients in our cohort showed a much lower proportion (17.40%) of A to T transversion ($T > A$) compared with the previous report¹⁷. C > A mutation accounts for 32.96% of the total mutation (Fig. 2A and Supporting Information Fig. S3). We further analyzed the contribution of signature 22 to the observed mutation spectra. Our data reveal that 41 out of 107 patients exhibited signature 22. However, only 9 patients displayed a dominant signature 22 in tumors, meaning that signature 22 was the most significant mutational pattern in 8.41% of 107

Table 1 Mass spectrometry parameters.

Ion pair	Q1 (Da)	Q3 (Da)	Time (ms)	DP (V)	CE (V)
dA-AAI	543.2	427.2	80	66	31
dA-AAI	543.2	395.2	80	55	65
IS	312.1	268.0	80	80	11

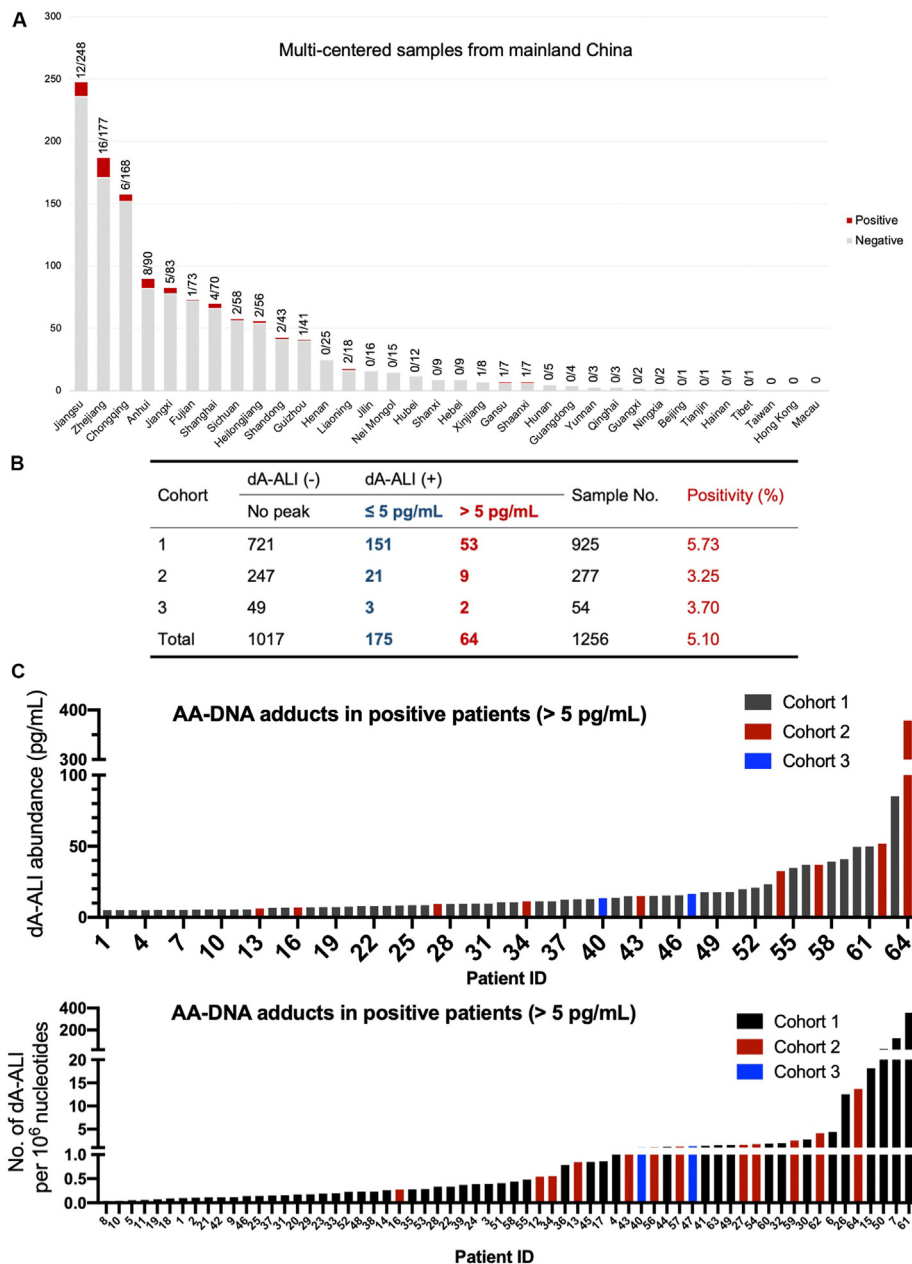


Figure 1 Low dA-ALI positive rate in HCCs from multi-centered samples in mainland China. (A) Distribution of HCC samples from 3 medical centers located in mainland China. The number of samples from different provinces was presented in bar chart. AAs positive patients were marked in red. The numbers above each bar show the ratio of AA positive patients to the total tested patients in each province. (B) Quantification results of dA-ALI detection in 1256 samples from above HCC patients. dA-ALI positive is defined as more than 5 pg dA-ALI per mL DNA. No peak in mass spectrometry analysis is defined as undetectable. (C) dA-ALI abundance in 64 AA–DNA adduct-positive patients was presented as pg/mL and dA-ALI per 10^6 nucleotides, relatively. Positive patients were marked as black, red and blue in cohort1, cohort 2 and cohort 3, respectively.

HCC samples (Fig. 2B). AA signature had a Pearson coefficient of 0.3795 among the signatures extracted (Supporting Information Fig. S4). Next, we examined the number of AA-associated mutation genes according to defined risk factors of HCC development or prognosis, namely, age at diagnosis, gender, alpha fetoprotein (AFP) level at diagnosis, liver cirrhosis, micro-vessel invasion (MVI) and tumor size. Of these, HCCs with liver cirrhosis or MVI have displayed a declined average number of AA-associated mutations. While there was no discrepancy of AA-associated mutation among the other variables (Supporting Information Fig. S5).

Among the 107 cases, 76 were divided into HBV positive group and 31 were HBV negative according to patient history and clinical test of HBV infection (Table S3). The panels of 30 most mutated genes between the two groups were slightly different (Fig. S2B). As expected, more driver gene mutation was observed in HBV positive group (Fig. S2C). However, there was no discrepancy in AA-associated gene mutation between these two groups (26.96 vs. 35.87, $P = 0.3943$) (Fig. 2C). The mutational spectra of HBV negative group showed a slight increase in T > A (20.14% vs. 16.20%) and a decrease in C > A (27.34% vs. 35.41%) (Fig. 2A and D). The correlation coefficients of AA mutational signature to

the observed mutation spectra were 0.5496 and 0.3006 in HBV negative group and HBV positive group, respectively (Fig. S4). For the 41 samples with signature 22, 11 out of 31 (35.48%) were HBV negative patients and 30 out of 76 (39.47%) were from HBV positive patients (Fig. 2E). The correlation coefficient between AA-associated mutation and total exonic mutation were 0.538 and 0.657 in HBV positive and HBV negative group relatively (Fig. 2F). Therefore, the above evidence indicate a relatively low proportion of AA mutational signature in HCCs, with no significant discrepancy between HBV positive and negative patients.

3.3. Lack of a positive link between AA–DNA adducts and AA mutational signature in human HCCs

Next, we compared the result of dA-ALI and AA mutational signature in each of the 107 patients, comprised of 23 dA-ALI detectable (marked as adduct positive group) and 84 dA-ALI undetectable patients (marked as adduct negative group). We found a slightly increased T > A mutation in adduct positive group (21.41%) than negative group (16.5%) or the overall mutation (17.4%) (Fig. 3A and B). The distribution of signature 22 in adduct positive and negative groups was similar (39.13% vs. 38.10%, $P = 0.928$) (Fig. 3C). Notably, in adduct positive group, 3 out of 23 (13.04%) patients had dominant signature 22. Whereas, 6 out of 32 (7.15%) patients in adduct negative group possessed dominant AA mutational signature ($P = 0.401$) (Fig. 3C). As to the number of AA signature associated mutations, we didn't observe an increase in adduct positive group (Fig. 3D). Additionally, the two groups exhibited a similar correlation of AA-associated mutations with total exonic mutations (Fig. 3E). More mutated driver genes were found in adduct negative patients, probably due to more individualized risk factors in this group (Fig. S2D and S2E). In general, adduct positive patients didn't show a predominant advantage in T > A mutation or more AA signature associated gene mutations.

3.4. Small doses of AAI did not cause liver tumorigenesis in adult mice in the long term

To further explore whether AAI could directly cause HCC in adulthood, we observed long-term effect of AAI on tumorigenesis in a mouse model. C57BL/6 mice at the age of 8 weeks were administered with varied doses of AAI (by gavage every other week) for a total of 8 months consecutively. Since a single dose of AAI (10 mg/kg) could cause kidney failure in rats within 2 months without obvious liver damage^{23,24}, the maximum dosage in our study was set at 3.0 mg/kg to avoid the mortality caused by severe kidney damage. CCl₄ was used to induce the inflammatory and fibrosis environment in liver (combined treatment) (Fig. 4A). AAI caused dose-dependent retarded weight gaining compared with the control (Supporting Information Fig. S6A). Creatinine (CRE) and urea (UREA) were used to monitor kidney function (Fig. S6B). Alanine aminotransferase (ALT) and aspartate aminotransferase (AST) were used to monitor liver damage. Mice treated with AAI alone or combined with CCl₄ have shown elevated ALT and AST in blood, demonstrating a certain level of liver injury (Fig. S6C and S6D). After the first dose of AAI for 4 months, no obvious abnormality in liver morphology could be observed (Fig. S6E). According to Sirius red staining, AAI merely resulted in (AAI alone treatment) or aggravated (combined treatment) fibrosis in mouse livers (Fig. S6E). We then prolonged the observation to 10 months and found bulky tumors formed in mouse forestomach in all the AAI treated groups (Fig. 4B). No macroscopic or microscopic

liver tumors could be detected in AAI alone groups (Fig. S6F). In CCl₄ combined treatment, a few tumors formed in each group (2/6 in control group, 1/5 in AAI 0.3 mg/kg and 2/6 in AAI 1.0 mg/kg, respectively), indicating CCl₄ other than AAI was responsible for liver tumorigenesis (Fig. 4C). Competing risk analysis suggested that forestomach carcinoma was responsible for the mortality caused by AAI in combined treatment groups (Fig. 4D). No kidney tumors were observed after 8 months of AAI treatment (Fig. 4E). However, the severity of kidney fibrosis increased with the dosage of AAI (Fig. 4E). In conclusion, although small doses of AAI could induce slight hepatocyte injury, it didn't cause liver tumorigenesis in the long term. Forestomach carcinoma is the main cause of death in this model.

3.5. AAI showed no additive effect in liver tumorigenesis in HBV transgenic mice

Since HBV infection is the leading risk factor of HCC in China, we further explored whether AAI could work with HBV to promote HCC in HBV transgenic (TgHBV) mouse models. In this study, we introduced two strains of TgHBV mice which expressed high-level HBV and detectable serum HBsAg, C57BL/6-TgHBV²⁵ and BALB/c-TgHBV, respectively²⁶. Mice were subjected to small doses of AAI administration (1.0 or 3.0 mg/kg) by gavage every other week, as indicated in Fig. 5A. Blood levels of ALT and AST were detected when they were sacrificed. Although C57BL/6-TgHBV mice showed a slightly higher baseline ALT, no obvious discrepancy of liver injury was detected between the two groups treated with AAI (Supporting Information Fig. S7A). For C57BL/6-TgHBV mice, no macroscopic tumors were observed after treatment of AAI alone for 10 months. Similar to wild type (WT) mice, there was no significant morphological abnormality or fibrosis caused by AAI in livers of C57BL/6-TgHBV mice (Fig. 5B). For CCl₄ combined treatment, few mice formed liver tumors in each group (2/6 in WT control group, 2/6 in WT combined treatment group, 2/6 in C57BL/6-TgHBV control group and 2/6 in C57BL/6-TgHBV combined treatment group). H&E and Sirius red also showed comparable liver fibrosis in each group, probably mainly caused by CCl₄ (Fig. 5C). In this model, forestomach carcinoma was formed in every animal of AAI treated groups after AAI treatment for 10 months (Fig. S7B). No kidney tumors were observed at this time point, while dose-dependent kidney fibrosis was validated in AAI-treated groups (Fig. S7C). Survival analysis revealed that in AAI alone groups, forestomach carcinoma caused dose-dependent mortality. In AAI (1.0 mg/kg) treated group, C57BL/6-TgHBV mice somehow showed slightly prolonged survival compared with WT group ($P = 0.03$, Fig. 5D). In combined treatment groups, AAI didn't decrease the life span of C57BL/6-TgHBV compared with WT mice (Fig. 5E).

Since BALB/c inbred mice were susceptible to CCl₄ induced liver fibrosis²⁷, they couldn't survive CCl₄ treatment for as long as two months. Therefore, we only observed the long-term impact of AAI exposure alone in this model. After AAI treatment for 10 months, no detectable liver tumors or notable liver fibrosis were observed in both BALB/c-WT and BALB/c-TgHBV mice (Fig. 5F). Although ALT and AST levels revealed a dose-dependent elevation in both BALB/c-TgHBV and control mice, there was no significant difference between the two groups (Fig. S7D). Every individual animal in AAI treated groups developed forestomach tumors (Fig. S7E), and no kidney tumors were detected at this time point (Fig. S7F). Survival analysis indicate that AAI caused a dose-dependent death related to forestomach carcinoma in both groups. Whereas, no significant

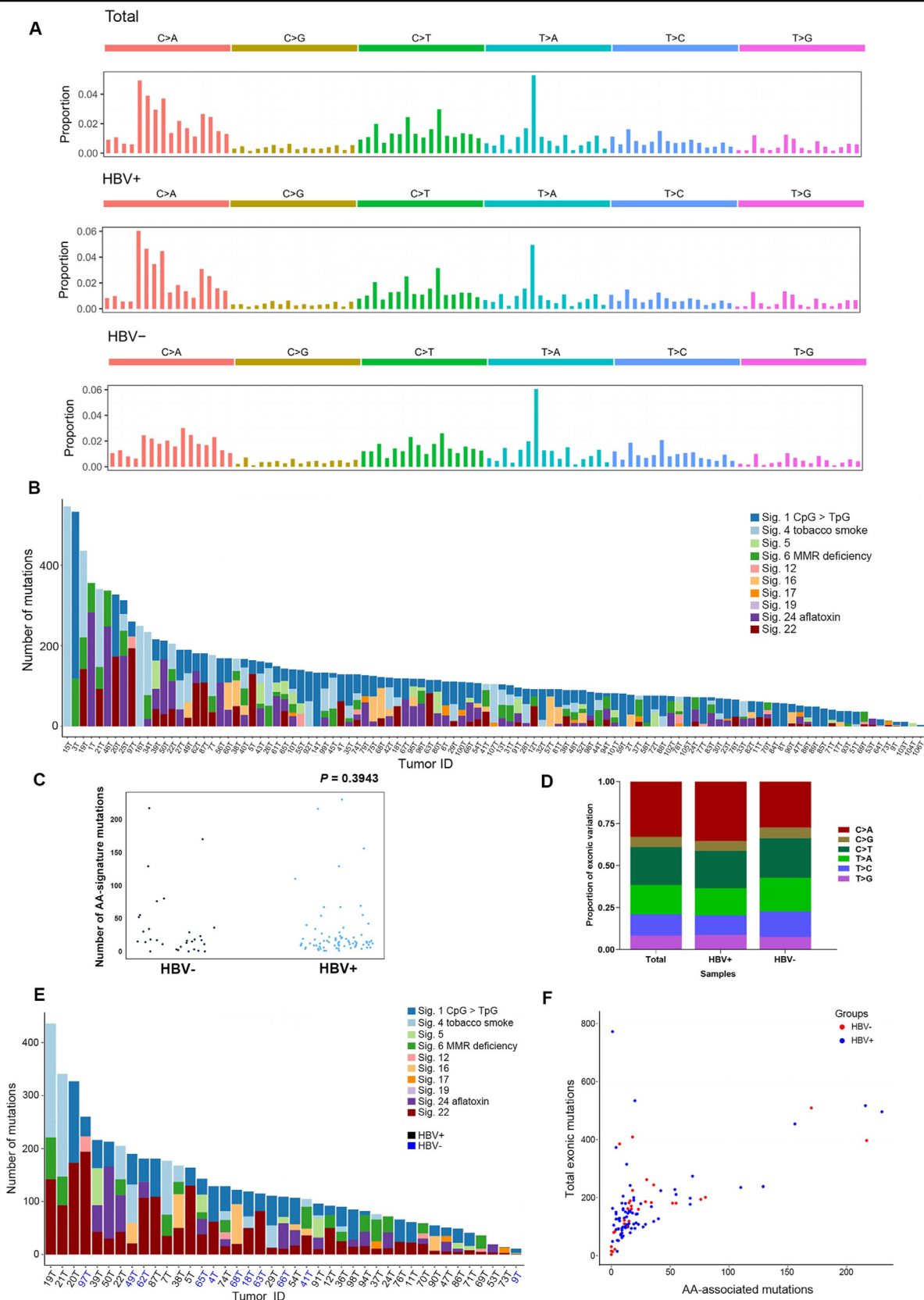


Figure 2 Low AA mutational signature was found in HCCs from EHBH cohort. (A) Average mutational spectra of 107 individual HCCs. Average mutational spectra of HBV positive ($n = 76$) and negative patients ($n = 31$) were presented. Each bar indicates the proportion of mutations in a particular trinucleotide context. (B) Estimated numbers of mutations contributed by each mutational signature in 107 HCC. Samples were listed according to total number of mutations. AA mutational signature is COSMIC signature 22. COSMIC signatures 4 and 24 reflect known exogenous risk factors for HCC: tobacco smoking and aflatoxin exposure, respectively. MMR, mismatch repair. (C) The comparison of AA signature mutations in HBV positive and HBV negative patients. $P = 0.3943$ (D) Exonic variation distribution of 107 patients, HBV positive ($n = 76$) and negative patients ($n = 31$). (E) Estimated numbers of mutations contributed by each mutational signature in patients with signature 22 ($n = 41$). Samples in HBV positive and negative group were marked in black and blue respectively. MMR, mismatch repair. (F) The correlation of total exonic mutations and AA-associated mutations were presented. HBV positive ($n = 76$) and negative group ($n = 31$) were marked in blue and red, relatively.

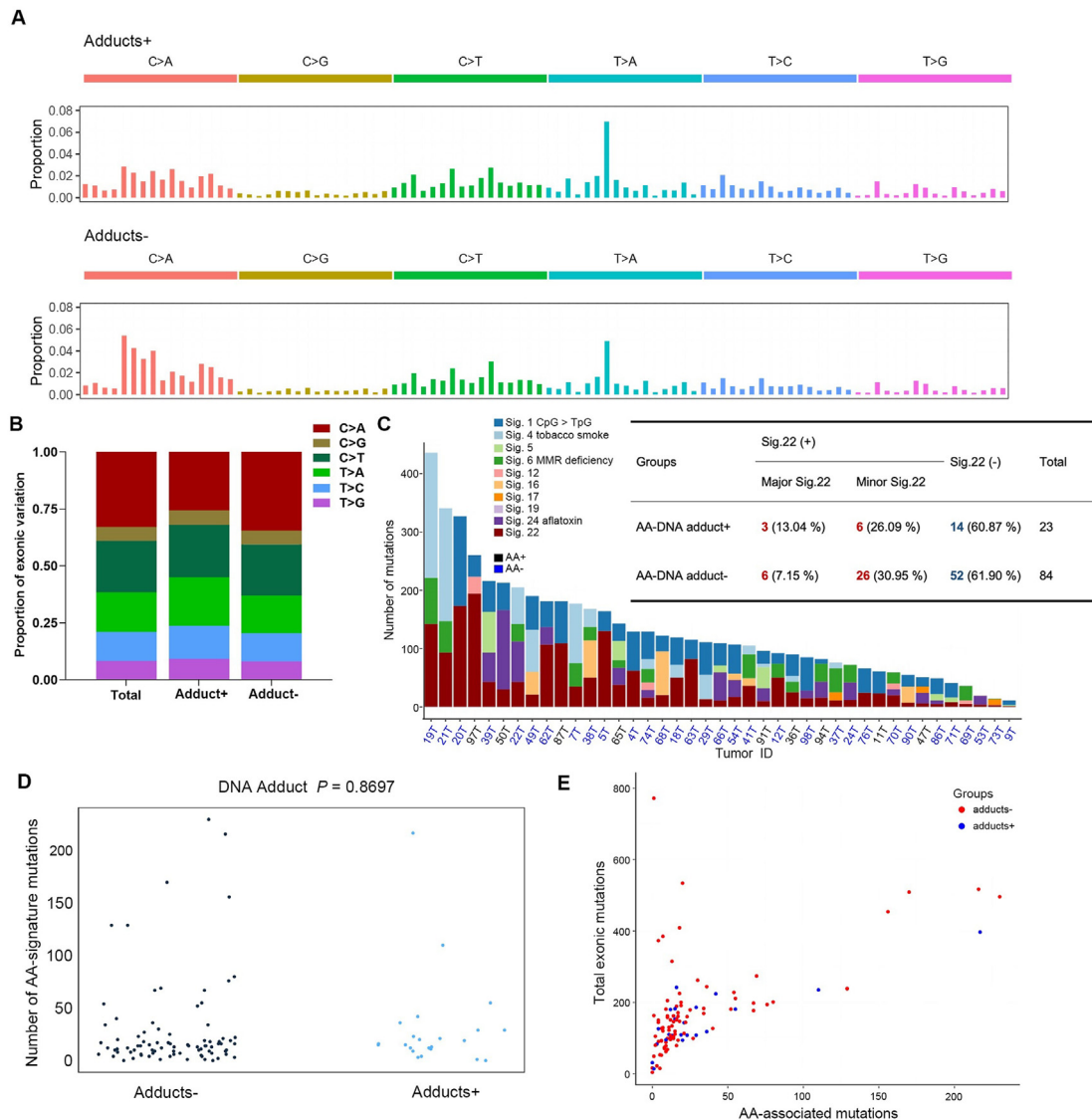


Figure 3 Lack of a positive link between AA–DNA adducts and AA mutational signature in human HCCs. (A) Average mutational spectra of AA–DNA adduct detectable group (Adduct+, $n = 23$) and AA–DNA adduct undetectable group (Adduct–, $n = 84$) were presented. No significant difference was detected in T > A mutation. (B) Exonic variation distribution of 107 patients, AA–DNA adduct detectable group and AA–DNA adduct undetectable group. (C) Estimated numbers of mutations contributed by each mutational signature in patients with signature 22 ($n = 41$). Samples in AA–DNA adduct detectable group and undetectable group were marked in black and blue respectively. MMR, mismatch repair. The table summarized the number of patients according to AA–DNA adduct detection and signature 22. Major Sig.22 means signature 22 was the dominant mutational signature of all the estimated signatures. Minor Sig.22 means signature 22 was detected in the sample but not the major estimated signature. Sig.22 (–) was identified as no estimated signature 22 in the sample. In AA–DNA adduct detectable group, 9 samples had signature 22, of which 3 samples had dominant signature 22. (D) The comparison of AA signature mutations in AA–DNA adduct detectable group and undetectable group. $P = 0.8697$. (E) The correlation of total exonic mutations and AA associated mutations were presented. AA–DNA adduct detectable group and undetectable group ($n = 31$) were marked in blue and red, relatively.

discrepancy was observed between the control group and BALB/c-TgHBV group under AAI treatment (Fig. 5G). Taken together, AAI didn't accelerate liver tumorigenesis under the pathological background of HBV infection in adult mice.

3.6. AAI could induce liver cancer when administered to infant mice

We further investigated if AAI could cause liver tumorigenesis when subjected to infant C57BL/6 mice. In this model, a well-defined liver carcinogen DEN was used as a positive control. A

single dose of DEN subjected to mice at the age of 14 days could induce severe tumorigenesis in mouse liver in 9 months²⁸. When DEN was combined with CCl₄, tumors could form as early as 4 months²⁹. DEN (20 mg/kg) or AAI (10 or 20 mg/kg) were administered to infant mice at 14 days after birth to compare its effect on inducing HCC (Fig. 6A). CCl₄ was used as mentioned before. Mice were sacrificed 10 months after AAI/DEN administration. As expected, severe tumor burden could be observed in DEN group (6/6), while fewer liver tumors were formed in AAI (20 mg/kg) group (6/7) and no macroscopic tumors could be observed in mice treated with AAI-10 mg/kg group (0/6) (Fig. 6B

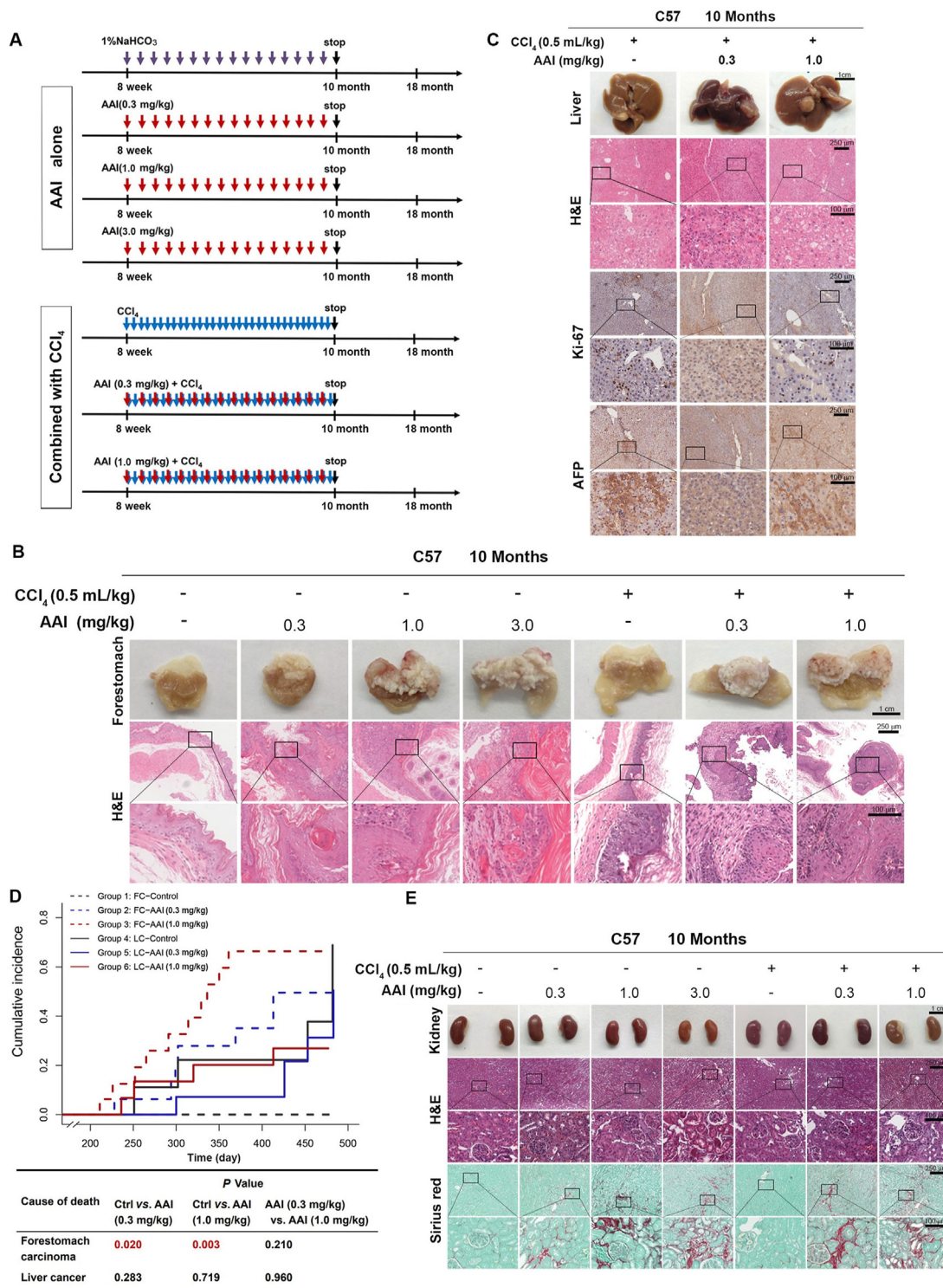


Figure 4 Small doses of AAI didn't cause liver tumorigenesis in adult mouse in long term. (A) Design of small doses AAI administration model in adult male C57BL/6 mice. AAI was given by gavage every other week with or without CCl₄ (0.5 mL/kg, once a week) at 8 weeks after birth. The red arrow represents AAI administration for 7 days a week. Blue arrow represents CCl₄ once a week. (B) Representative images of macroscopic (scale bars, 1 cm) and H&E staining (scale bars, 100 or 250 μm) of forestomach in AAI alone groups and AAI combined treatment groups at 10 months were presented. (C) Representative images of macroscopic (scale bars, 1 cm), H&E staining (scale bars, 100 or 250 μm), and IHC staining (AFP and Ki-67, scale bars, 100 or 250 μm) of liver samples in AAI combined treatment groups at 10 months were presented. (D) Competing survival analysis has compared the mortality caused by forestomach carcinoma and liver cancer in AAI combined with CCl₄ treatment groups and control group. The table summarized P values of different doses of AAI groups under two causes of death. AAI caused a dose-dependent death due to forestomach carcinoma. No significant difference in liver cancer-related death between different doses of AAI treatment was found. (E) Representative images of macroscopic (scale bars, 1 cm), H&E staining (scale bars, 100 or 250 μm), and Sirius red staining (scale bars, 100 or 250 μm) of kidney in AAI alone groups and AAI combined treatment groups at 10 months.

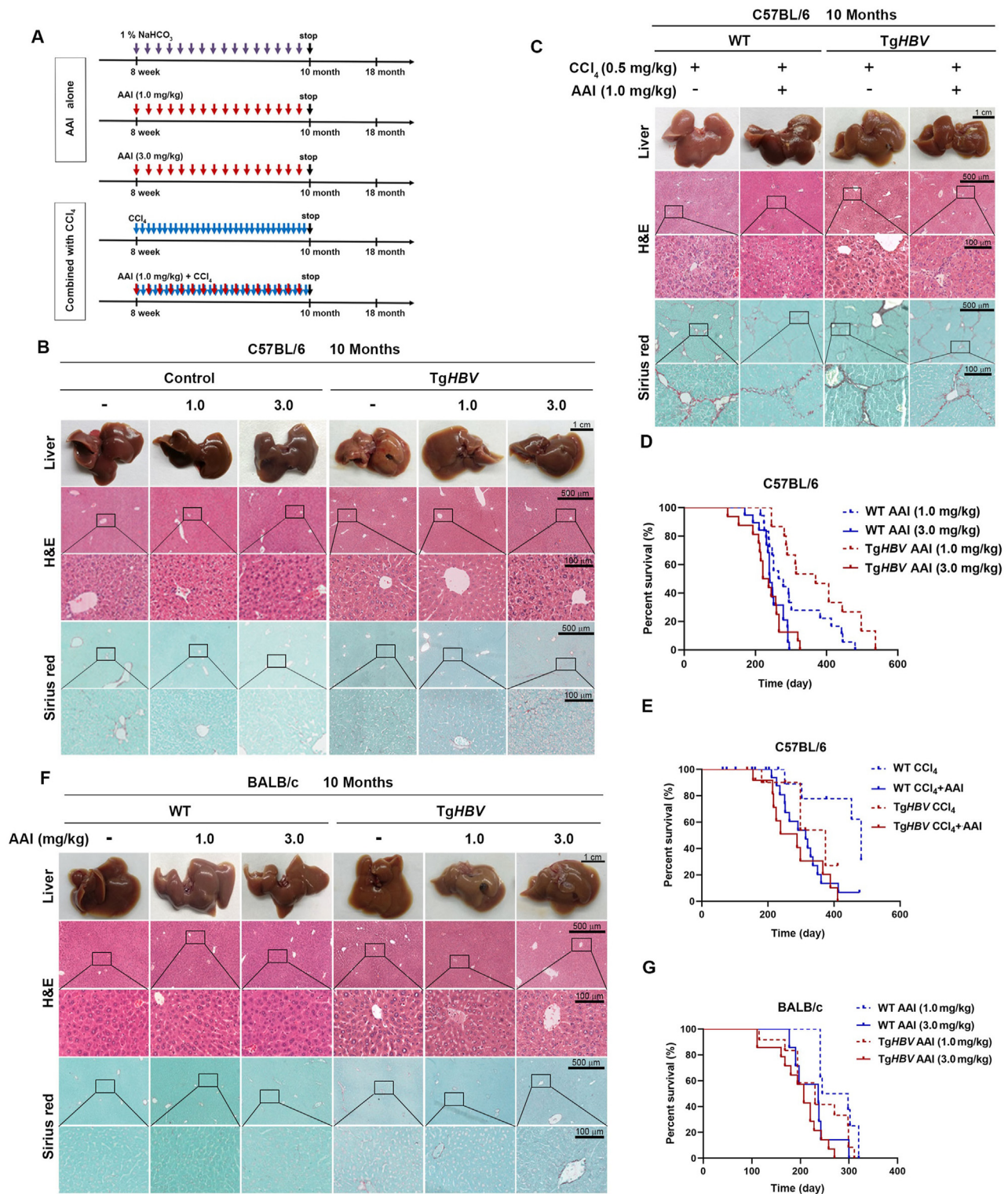


Figure 5 AAI showed no additive effect with HBV in the development of HCC. (A) Design of AAI administration in WT and *TgHBV* mice model. NaHCO_3 was served as control. AAI was subjected to mice at the age of 8 weeks by gavage for 8 months. AAI combined CCl_4 treatment groups received a single shot of CCl_4 intraperitoneally every other week. (B) Representative images of macroscopic (scale bars, 1 cm), H&E staining (scale bars, 100 or 500 μm) and Sirius red (scale bars, 100 or 500 μm) of liver samples in AAI treatment groups of C57BL/6-WT and C57BL/6-*TgHBV* mice at 10 months. (C) Representative images of macroscopic (scale bars, 1 cm), H&E staining (scale bars, 100 or 500 μm) and Sirius red (scale bars, 100 or 500 μm) of liver samples in AAI combined CCl_4 treatment groups of C57BL/6-WT and C57BL/6-*TgHBV* mice at 10 months. (D) Survival rate of C57BL/6-WT and C57BL/6-*TgHBV* mice in AAI alone treatment groups were calculated and presented in charts. (E) Survival rate of C57BL/6-WT and C57BL/6-*TgHBV* mice in combined CCl_4 treatment groups were calculated and presented in charts. (F) Representative images of macroscopic (scale bars, 1 cm), H&E staining (scale bars, 100 or 500 μm) and Sirius red (scale bars, 100 or 500 μm) of liver samples in AAI alone treatment groups of BALB/c-WT and BALB/c-*TgHBV* mice at 10 months. (G) Survival rate of BALB/c-WT and BALB/c-*TgHBV* mice in AAI treatment groups were calculated and presented in the chart.

and D). When the observation was extended to 16 months, tumor burden in AAI (10 mg/kg) group was comparable to DEN treated group at 10 months (Supporting Information Fig. S8A). These data indicate that the same dose of AAI treatment could impose a slightly weaker genotoxic effect than DEN in liver. In CCl₄ combined groups, AAI (10 mg/kg) exhibited a similar effect of DEN with comparable tumor numbers and microscopic pathological morphology (Fig. 6C). Mice treated with AAI showed a significant dose-dependent increase in tumor burdens per liver. Mice treated with AAI (20 mg/kg) even formed more tumors per liver than DEN injected mice (Fig. 6D). No forestomach tumors were detected at the above time points (Fig. S8B–S8E). In comparison, a single dose of AAI could cause kidney fibrosis (Fig. S8C and S8D) and a slight increase in blood CRE and UREA (Fig. S8F). We've also observed similar results in C57BL/6-TgHBV mice with the above treatment (Fig. S8G). Furthermore, when AAI (3.0 mg/kg) was supplemented every other week in DEN plus CCl₄ model, started one week after the first dose of CCl₄ till the mice were sacrificed, additional AAI treatment didn't cause more liver tumor formation in WT and C57BL/6-TgHBV mice (Fig. 6E and F). Therefore, this model demonstrated that AAI could cause liver tumorigenesis when administered to infant mice.

3.7. AAI induced AA–DNA adducts in a dose-dependent manner instead of AA mutational signature in target organs

From the previous data, positive AA–DNA adducts in HCC patients didn't necessarily lead to dominant AA mutational signature. Therefore, we further validated if AA–DNA adducts or AA mutational signature was correlated to AAI exposure in the above animal models, since AAI consumption for each animal was traceable and countable. Our data reveal a dose-dependent increase of dA-ALI in liver and kidney (Fig. 7A). In CCl₄ combined treatment group, kidney still exhibited the most abundant dA-ALI as in AAI alone groups (Fig. 7B). Forestomach tumor has shown a rather low accumulation of dA-ALI, probably because that massive replication of tumor cells diluted the proportion of genomic AA–DNA adducts³⁰. Therefore, dA-ALI level in forestomach might be higher before the tumor formed. To explore dA-ALI distribution before tumor formed, C57BL/6 mice aged at 8 weeks were given AAI (3.0 mg/kg) every other week for one month or two months before sacrificed. Our data show that the short-term administration of AAI also caused massive dA-ALI formation in kidney other than liver and forestomach (Fig. 7C). In two TgHBV mouse models, dA-ALI formation exhibited a dose-dependent manner in liver, but was still most abundant in kidney (Supporting Information Fig. S9A). dA-ALI level was comparable between WT and TgHBV mice under the same dosage of AAI (Fig. S9B). In infant model, kidney displayed the most abundance of dA-ALI, although it declined as the mice aged since they only received a single shot of AAI at the age of 14 days (Fig. 7D). Therefore, we could safely conclude that dA-ALI was positively correlated with the AAI exposure in target organs and kidney was the most vulnerable organ for dA-ALI formation.

We further investigated AA mutational signature in samples of long-term and short-term models. WGS revealed a dominant T > A mutation in forestomach tumors in adult mice. A slight increase of T > A mutation could also be observed in liver, compared with the control group (Fig. 7E). In the short term (2 months) AA exposure model, T > A mutation was significantly elevated in forestomach (Fig. 7F). However, it is worth noticing that even though kidney was the main target for AA–DNA adduct formation, T > A

mutation was not significantly increased in kidney when no tumor was formed (Fig. 7F). In infant model, massive T > A mutation occurred in liver tumors and para-tumors instead of kidney, where the dA-ALI level was relatively higher (Fig. 7G). Taken together, AA–DNA adduct was positively correlated with the consumption of AAI in target organs. However, AA–DNA adduct may not necessarily lead to T > A mutation.

4. Discussion

Liver cancer ranks as the second leading cause of cancer-related death in China¹⁵. HCC accounts for 85%–90% of all cases with poor prognosis. High risk factors of HCC comprised of chronic hepatitis (B/C), aflatoxin contamination, nonalcoholic steatohepatitis, etc. The success of antiviral therapy on HBV and anti-HBV vaccine has greatly contributed to decreasing the prevalence of HBV-related HCC. Therefore, identifying chemical compounds that pose great threat to HCC is an effective approach for tumor prevention.

In this study, we demonstrate that AAs exposure was not the main cause of HCC in our cohorts, which was contradictory to a previous report. The conclusion of the previous report¹⁷ was mainly based on WGS analysis of AA mutational signature in HCCs from Taiwan area of China via a newly developed software mSigAct (mutational signature activity). However, another group of researchers re-measured the AA signature in Chinese samples from datasets and only got AA signature in 5 out of 88 HCCs compared with 42 out of 88 patients from the previously published paper³¹. Researchers further measured AA signature frequencies with HCC from TCGA dataset and found that only 10.2% (19/187) of Asians had AA signatures. Therefore, they indicated there might be more errors in mSigAct when the proportion of AA signature mutation is not high³¹. Besides, whether these patients had AA exposure history was unclear. Another study evaluated the effect of AA exposure on human liver cancers³². In two mainland China liver cancer datasets they have selected, AA signature exposure greater than 0 were 17% (52/313)³³ and 11% (11/103)¹⁷, respectively. Moreover, a recent study investigated somatic mutant clonal events of 120 patients with urothelial cell carcinoma and found that AA mutagenesis was more prevalent in females than in males in urothelial samples³⁴. The gender bias is contrary to the incidence of liver cancer, which is male dominant. In our study, we observed a lower A to T transversion (17.40%) in the mutation spectra of 107 patients (Fig. 2A) than the previous report indicated¹⁷. 41 out of 107 HCCs have displayed signature 22 and only 9 patients (8.41%) showed dominant signature 22 (Fig. 2B). Thus, based on our data, we believe that the evidence of AA exposure widely implicated in mainland China HCC was not as convincing as the previous report indicated. However, we have to admit that the limited number of samples in our study was not enough to draw the conclusion about the overall mutational spectra of HCCs in mainland China. But it's noticeable that no case report has linked AAI to HCC in mainland China by far.

Previous studies lacked evidence of dA-ALI examination in a large amount of HCC patients. In this study, by using the improved method to quantify dA-ALI¹⁹ in HCC FFPE samples from 3 medical centers in mainland China, we have found that dA-ALI was detectable in 239 (19.03%) samples. However, only 64 samples (5.10%) could be identified as AAI positive exposure (Fig. 1B). The feasibility of yielding DNA from FFPE tissue may cause sampling bias derived from the varied time interval between tissue procurement and formalin fixation, thereby possibly

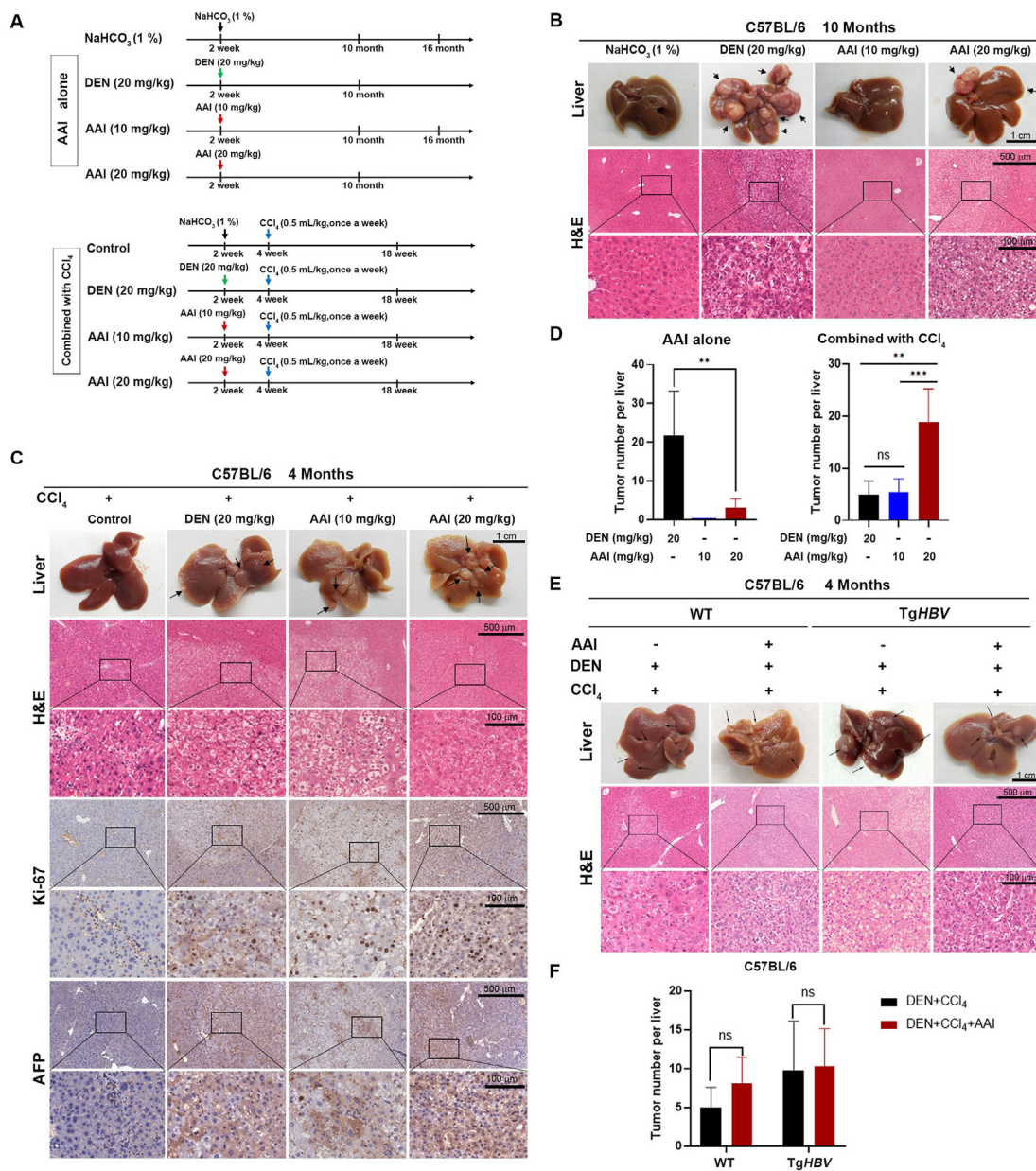


Figure 6 AAI induced liver cancer when administered to infant C57BL/6 mice. (A) Design of AAI administration in infant C57BL/6 mice model. NaHCO₃ was served as negative control and DEN (20 mg/kg) as the positive control. One single shot of AAI (10 or 20 mg/kg) or DEN was injected intraperitoneally at 14 days after birth. CCl₄ (0.5 mL/kg) was used to accelerate tumorigenesis once a week for 14 weeks in combined treatment groups. (B) Representative images of macroscopic (scale bars, 1 cm) and H&E staining (scale bars, 100 or 500 μ m) of liver samples in AAI alone treatment groups at 10 months. The black arrows point at tumors formed on liver. (C) Representative images of macroscopic (scale bars, 1 cm), H&E staining (scale bars, 100 or 500 μ m), and IHC staining (Ki-67 and AFP; scale bars, 100 or 500 μ m) of liver samples in control, DEN and AAI combined CCl₄ treatment groups at 4 months. The black arrows point at tumors formed on liver. (D) Tumor number per liver in DEN group. AAI alone treatment (left) and AAI combined treatment groups (right) were calculated and presented. (E) Representative images of macroscopic (scale bars, 1 cm), H&E staining (scale bars, 100 or 500 μ m) of liver samples in WT and C57BL/6-TgHBV which AAI (3.0 mg/kg) was supplemented every other week for DEN combined with CCl₄ treatment groups at 4 months. (F) Tumor number per liver of WT and C57BL/6-TgHBV mice in Fig. 6E were calculated and presented. Values are presented as mean \pm SD; * P < 0.05; ** P < 0.01; *** P < 0.001; ns, no significance.

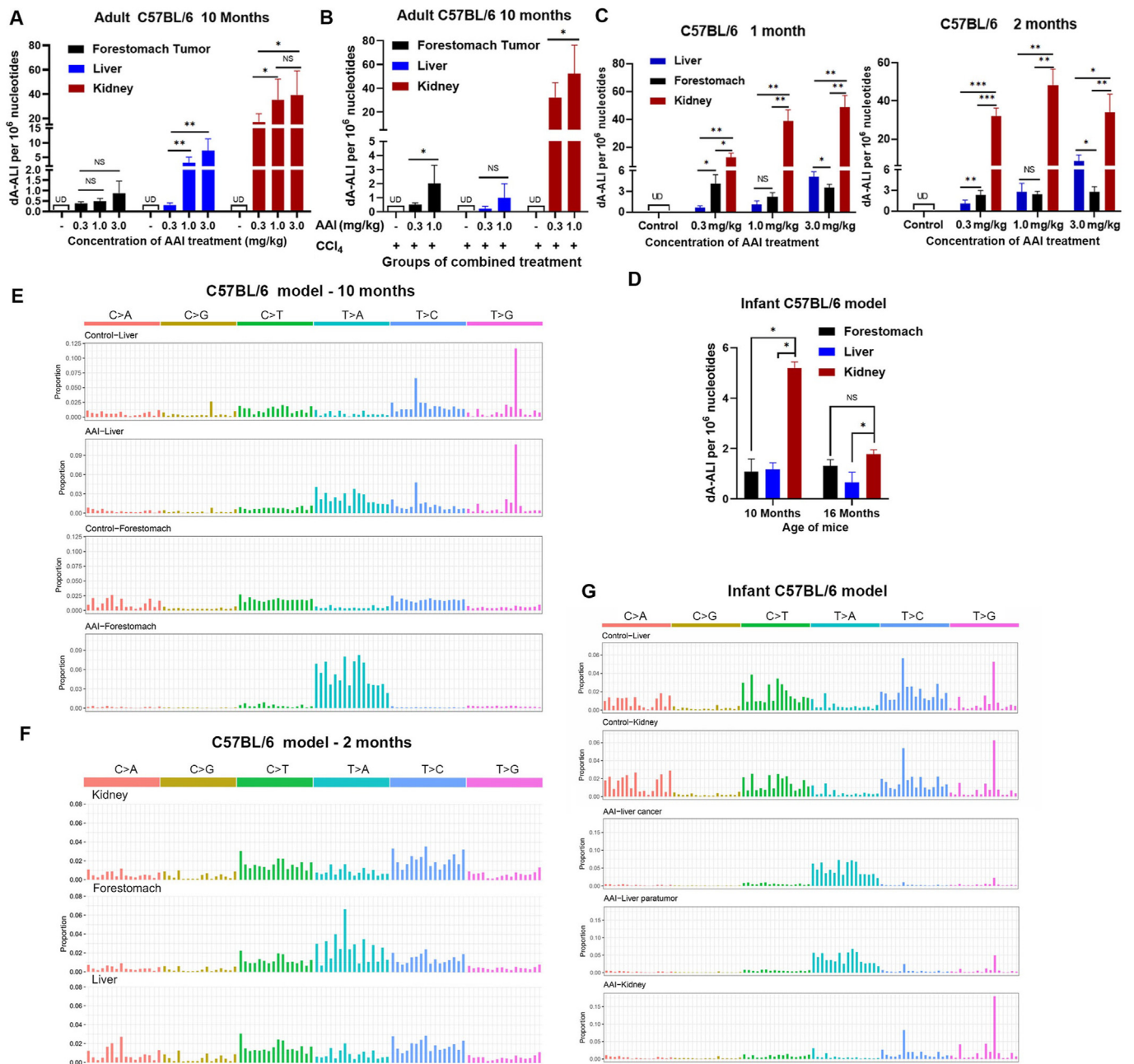


Figure 7 AAI induced AA–DNA adducts in a dose-dependent manner instead of AA mutational signature in target organs. (A) AA–DNA adduct was detected in liver, forestomach tumor and kidney samples of mice in adult C57BL/6 model with indicated doses of AAI gavage for 8 months. The results are presented as dA-ALI per 10⁶ nucleotides. UD: undetected. (B) dA-ALI was detected in liver, forestomach tumor and kidney samples of mice in adult C57BL/6 model with AAI combined CCl₄ treatment for 8 months. The results are presented as dA-ALI per 10⁶ nucleotides. UD: undetected. (C) C57BL/6 WT mice at the age of 8 months were subjected to AAI (3.0 mg/kg) by gavage every other week for 1 month (left) or 2 months (right) before sacrificed. dA-ALI quantification was determined in liver, forestomach and kidney and presented as dA-ALI per 10⁶ nucleotides. (D) dA-ALI quantification was determined in liver, forestomach and kidney samples in infant mice model sacrificed at the indicated time points. (E) Mutational spectra of liver and forestomach in C57BL/6 mice with AAI alone treatment for 8 months was determined by WGS analysis. Mice with NaHCO₃ by gavage for 8 months were served as control. (F) Mutational spectra of liver and kidney in infant mice model at the age of 16 months was determined by WGS analysis. Mice with a single shot of NaHCO₃ intraperitoneally at the age of 14 day served as the control. (G) Mutational spectra of kidney, forestomach and kidney of C57BL/6 mice with AAI treated by gavage for 2 months. Values are presented as mean ± SD; **P* < 0.05; ***P* < 0.01; ****P* < 0.001; NS, no significance.

impacting the measurement of carcinogen DNA adducts³⁵. However, AAI–DNA adducts were chemically stable to the conditions of DNA and were present in the oligomers¹⁰, suggesting the fixation procession of samples has little effect on the DNA adducts quantification. One study reported that AAI adducts in human kidney FFPE tissues for up to 9 years are recovered in high yield and their levels are comparable with those in matching freshly frozen tissues³⁶. Therefore, the detection of AAI–DNA adducts in FFPE samples from different sources was acceptable for AAI–DNA adducts measurement.

In this study, we also compared the role of AAI on liver tumorigenesis when it was subjected to mice at their infancy or adulthood. In contrast, a shot of AAI (20 mg/kg) at the age of 14 days plus CCl₄ treatment could induce heavy tumor burden, which was comparable to the effect of DEN. Long-term administration of AAI in small doses barely promoted liver tumors until the age of 10 months. The main cause of death was forestomach carcinoma. The following reasons could be responsible for the discrepancy. (1) AAI was administered to infant mice i.p. and to adult mice by gavage. With i.p. injection, drug is absorbed into the mesenteric blood supply that is carried directly to the liver and subject to hepatic first-pass metabolism, leading to even more liver injury than other routes. That's why DEN is commonly administered between 12 and 15 days of age by a single intraperitoneal injection, given the liver is the primary target to the exposed chemical compounds and the key detoxification enzymes (cytochrome P450) increases and reaches its peak activity between the 7th and 15th day of age and then decreases³⁷. However, we should notice that oral route instead of intraperitoneal injection is the authentic way of uptaking AAs in human. (2) The enzymes responsible for detoxifying the bio-activation of AAI to form DNA adducts were compromised in infant mice, which makes them vulnerable target for AAI induced damage. The enzyme activities and mRNA expression of various phase I and phase II metabolic enzymes that contributed to the detoxification of AAI in the liver of 2-week-old mice are lower than adult mice^{38,39}. (3) The high proliferation rate of hepatocytes in infant mice is conducive to cumulative gene mutation caused by carcinogen. The gene mutation caused by carcinogen could be cloned and amplified with cell proliferation^{40,41}. Due to the high proliferation and renewal of hepatocytes around the age of 15 days, the susceptibility of infant mice to hepatocellular carcinogenesis is much higher than in adulthood, laying seeds for later liver cancer.

AA–DNA adduct is a well-known biomarker for AA exposure since it could persist for many years^{11–13,42}. Our data show that AA–DNA adduct could be detected in a dose-dependent manner and kidney exhibited the highest dA–ALI level among these three organs, which was in accord to previous reports, since organ susceptibility of AAI toxicity has long been validated⁴³. However, no quantitative correlation exists between the level of DNA adduct formation and carcinogenicity in different organs. We assumed that DNA damage repair capacity resulted in the discrepant removal efficacy of DNA adduct that can cause mutations and later give rise to cancer. This theory also explained why HCC patients with positive AA–DNA adducts from our cohort didn't show a significant A–T transversion in genome. Besides, whether these patients with detectable dA–ALI have consumed AA-containing drugs or if AA consumption occurred before or after HCC diagnosis was also absent. Although the previous report suggested that the quantity of DNA adducts formed by a DNA-reactive compound is not a carcinogenicity predictor⁴⁴, whether there was a threshold for dA–ALI to cause gene mutation is worth further investigation.

5. Conclusions

Taken together, our study demonstrated that AAs were not the main cause of liver cancer in adulthood. Also, more evidence was needed to demonstrate AA exposure as the main cause of HCC in mainland China. However, due to their genetic toxicity, the use of AAs-containing drugs should be taken with more caution, especially in the underage group and patients with liver malfunction.

Acknowledgments

We appreciate the support from Shanghai Key Laboratory of Hepatobiliary Tumor Biology and Ministry of Education Key Laboratory on Signaling Regulation and Military Key Laboratory and Targeting Therapy of Liver Cancer, Second Military Medical University, Shanghai, China. We want to thank People's Liberation Army 307 Hospital (China) for the HCC samples provided. We appreciate the valuable suggestions provided by Dr. Yang Luan from Shanghai Jiaotong University (Shanghai, China). We also want to thank Liang Tang, Shan-Hua Tang, Lin-Na Guo and Dan Cao for their technical assistance. This project was supported by National Major Scientific and Technological Special Project for "Significant New Drugs Development" (2018ZX09101002, 2018ZX09101002-001-001, and 2018ZX09101002-001-002, China). It's also sponsored by National Natural Science Foundation of China (81830054, 91859205, 81988101, 81722034, and 81802878), Shanghai Pujiang Program (2019PJD059, China), Shanghai Sailing Program (18YF1400200, China) and Key Discipline Project of Shanghai Municipal Education Commission (201901070007E00065, China).

Author contributions

Conception and design: Shuzhen Chen, Wen Wen and Hongyang Wang; Development of methodology: Shuzhen Chen and Yaping Dong; Acquisition of data (provided animals, provided facilities, etc.): Shuzhen Chen, Yaping Dong, Lingyan Xu, Qiqi Cao, and Zhecai Fan; Synthesis and identification of dA–ALI: Xinming Qi and Guozhen Xin; Collection of epidemiological data: Zhaofang Bai, Chunyu Wang, Huisi He, and Zhichao Jin; Collection of patients' sample and clinical data: Yaping Dong, Tao Luo, Jiao Wang, Jia Ge, Lei Chen, Xiaohe Xiao, and Xiuwu Bian; Patients' follow-up and data sorting: Huisi He, Zhixuan Li, and Qiqi Cao; Analysis and interpretation of data (*e.g.*, statistical analysis, biostatistics, computational analysis): Shuzhen Chen, Qiqi Cao, Yaping Dong, Zhichao Jin, and Huisi He; Writing, review, and/or revision of the manuscript: Qiqi Cao, Shuzhen Chen, Wen Wen, and Hongyang Wang; Administrative, technical, or material support (*i.e.*, reporting or organizing data, constructing databases): Zhecai Fan, Huisi He, and Yishan Zhong; Study supervision: Jin Ren, Wen Wen, and Hongyang Wang.

Conflicts of interest

The authors have no conflict of interest to declare.

Appendix A. Supporting information

Supporting data to this article can be found online at <https://doi.org/10.1016/j.apsb.2021.11.011>.

References

- Yang HY, Chen PC, Wang JD. Chinese herbs containing aristolochic acid associated with renal failure and urothelial carcinoma: a review from epidemiologic observations to causal inference. *BioMed Res Int* 2014;569325. 2014.
- Vanherweghem LJ. Misuse of herbal remedies: the case of an outbreak of terminal renal failure in Belgium (Chinese herbs nephropathy). *J Alternative Compl Med* 1998;4:9–13.
- Vanherweghem JL, Depierreux M, Tielemans C, Abramowicz D, Dratwa M, Jadoul M, et al. Rapidly progressive interstitial renal fibrosis in young women: association with slimming regimen including Chinese herbs. *Lancet* 1993;341:387–91.
- Nortier JL, Martinez MC, Schmeiser HH, Arlt VM, Bieler CA, Petein M, et al. Urothelial carcinoma associated with the use of a Chinese herb (*Aristolochia fangchi*). *N Engl J Med* 2000;342:1686–92.
- Chen CH, Dickman KG, Moriya M, Zavadil J, Sidorenko VS, Edwards KL, et al. Aristolochic acid-associated urothelial cancer in Taiwan. *Proc Natl Acad Sci U S A* 2012;109:8241–6.
- Poon SL, Huang MN, Choo Y, McPherson JR, Yu W, Heng HL, et al. Mutation signatures implicate aristolochic acid in bladder cancer development. *Genome Med* 2015;7:38.
- Shibutani S, Dong H, Suzuki N, Ueda S, Miller F, Grollman AP. Selective toxicity of aristolochic acids I and II. *Drug Metab Dispos* 2007;35:1217–22.
- Sato N, Takahashi D, Chen SM, Tsuchiya R, Mukoyama T, Yamagata S, et al. Acute nephrotoxicity of aristolochic acids in mice. *J Pharm Pharmacol* 2004;56:221–9.
- Schmeiser HH, Scherf HR, Wiessler M. Activating mutations at codon 61 of the c-Ha-ras gene in thin-tissue sections of tumors induced by aristolochic acid in rats and mice. *Cancer Lett* 1991;59:139–43.
- Attaluri S, Bonala RR, Yang IY, Lukin MA, Wen Y, Grollman AP, et al. DNA adducts of aristolochic acid II: total synthesis and site-specific mutagenesis studies in mammalian cells. *Nucleic Acids Res* 2010;38:339–52.
- Grollman AP, Shibutani S, Moriya M, Miller F, Wu L, Moll U, et al. Aristolochic acid and the etiology of endemic (Balkan) nephropathy. *Proc Natl Acad Sci U S A* 2007;104:12129–34.
- Schmeiser HH, Nortier JL, Singh R, Gamboa da Costa G, Sennesael J, Cassuto-Viguiere E, et al. Exceptionally long-term persistence of DNA adducts formed by carcinogenic aristolochic acid I in renal tissue from patients with aristolochic acid nephropathy. *Int J Cancer* 2014;135:502–7.
- Sidorenko VS, Yeo JE, Bonala RR, Johnson F, Schärer OD, Grollman AP. Lack of recognition by global-genome nucleotide excision repair accounts for the high mutagenicity and persistence of aristolactam–DNA adducts. *Nucleic Acids Res* 2012;40:2494–505.
- Poon SL, Pang ST, McPherson JR, Yu W, Huang KK, Guan P, et al. Genome-wide mutational signatures of aristolochic acid and its application as a screening tool. *Sci Transl Med* 2013;5:197ra01.
- Villanueva A. Hepatocellular carcinoma. *N Engl J Med* 2019;380:1450–62.
- Huang J, Deng Q, Wang Q, Li KY, Dai JH, Li N, et al. Exome sequencing of hepatitis B virus-associated hepatocellular carcinoma. *Nat Genet* 2012;44:1117–21.
- Ng AWT, Poon SL, Huang MN, Lim JQ, Boot A, Yu W, et al. Aristolochic acids and their derivatives are widely implicated in liver cancers in Taiwan and throughout Asia. *Sci Transl Med* 2017;9:412.
- Gao Q, Zhu H, Dong L, Shi W, Chen R, Song Z, et al. Integrated proteogenomic characterization of HBV-related hepatocellular carcinoma. *Cell* 2019;179:561–77. e22.
- Wang X, Song J, Dong Y, Hu L, Chen X, Yang F, et al. Qualitative and quantitative bioanalytical methods validation of aristolochic acid DNA adducts and application in human formalin-fixed paraffin-embedded hepatocellular carcinoma tissues. *bioRxiv* 2020. Available from: <https://www.biorxiv.org/content/10.1101/2020.08.20.260331v2>.
- Stiborova M, Arlt VM, Schmeiser HH. DNA adducts formed by aristolochic acid are unique biomarkers of exposure and explain the initiation phase of upper urothelial cancer. *Int J Mol Sci* 2017;18:2144.
- Lin H, Tang X, Shen P, Zhang D, Wu J, Zhang J, et al. Using big data to improve cardiovascular care and outcomes in China: a protocol for the Chinese Electronic health Records Research in Yinzhou (CHERRY) Study. *BMJ Open* 2018;8:e019698.
- Cancer Genome Atlas Research Network. Electronic address wbe, Cancer Genome Atlas Research N. Comprehensive and integrative genomic characterization of hepatocellular carcinoma. *Cell* 2017;169:1327–1341.e23.
- Zhao YY, Zhang L, Mao JR, Cheng XH, Lin RC, Zhang Y, et al. Ergosta-4,6,8(14),22-tetraen-3-one isolated from *Polyporus umbellatus* prevents early renal injury in aristolochic acid-induced nephropathy rats. *J Pharm Pharmacol* 2011;63:1581–6.
- Rosenquist TA, Einolf HJ, Dickman KG, Wang L, Smith A, Grollman AP. Cytochrome P450 1A2 detoxicates aristolochic acid in the mouse. *Drug Metab Dispos* 2010;38:761–8.
- Tian X, Zhao C, Zhu H, She W, Zhang J, Liu J, et al. Hepatitis B virus (HBV) surface antigen interacts with and promotes cyclophilin a secretion: possible link to pathogenesis of HBV infection. *J Virol* 2010;84:3373–81.
- Ren J, Wang L, Chen Z, Ma ZM, Zhu HG, Yang DL, et al. Gene expression profile of transgenic mouse kidney reveals pathogenesis of hepatitis B virus associated nephropathy. *J Med Virol* 2006;78:551–60.
- Hillebrandt S, Goos C, Matern S, Lammert F. Genome-wide analysis of hepatic fibrosis in inbred mice identifies the susceptibility locus Hfib1 on chromosome 15. *Gastroenterology* 2002;123:2041–51.
- Vesselinovitch SD, Mihailovich N. Kinetics of diethylnitrosamine hepatocarcinogenesis in the infant mouse. *Cancer Res* 1983;43:4253–9.
- Uehara T, Pogribny IP, Rusyn I. The DEN and CCl₄-induced mouse model of fibrosis and inflammation-associated hepatocellular carcinoma. *Curr Protoc Pharmacol* 2014;66:14301–10.
- Yun BH, Rosenquist TA, Sidorenko V, Iden CR, Chen CH, Pu YS, et al. Biomonitoring of aristolactam–DNA adducts in human tissues using ultra-performance liquid chromatography/ion-trap mass spectrometry. *Chem Res Toxicol* 2012;25:1119–31.
- Ji X, Feng G, Chen G, Shi T. Lack of correlation between aristolochic acid exposure and hepatocellular carcinoma. *Sci China Life Sci* 2018;61:727–8.
- Lu ZN, Luo Q, Zhao LN, Shi Y, Wang N, Wang L, et al. The mutational features of aristolochic acid-induced mouse and human liver cancers. *Hepatology* 2020;71:929–42.
- Zou S, Li J, Zhou H, Frech C, Jiang X, Chu JS, et al. Mutational landscape of intrahepatic cholangiocarcinoma. *Nat Commun* 2014;5:5696.
- Li R, Du Y, Chen Z, Xu D, Lin T, Jin S, et al. Macroscopic somatic clonal expansion in morphologically normal human urothelium. *Science* 2020;370:82–9.
- Yun BH, Rosenquist TA, Nikolic J, Dragicevic D, Tomic K, Jelakovic B, et al. Human formalin-fixed paraffin-embedded tissues: an untapped specimen for biomonitoring of carcinogen DNA adducts by mass spectrometry. *Anal Chem* 2013;85:4251–8.
- Jelakovic B, Karanovic S, Vukovic-Lela I, Miller F, Edwards KL, Nikolic J, et al. Aristolactam–DNA adducts are a biomarker of environmental exposure to aristolochic acid. *Kidney Int* 2012;81:559–67.
- Rao KV, Vesselinovitch SD. Age- and sex-associated diethylnitrosamine dealkylation activity of the mouse liver and hepatocarcinogenesis. *Cancer Res* 1973;33:1625–7.
- Peng L, Cui JY, Yoo B, Gunewardena SS, Lu H, Klaassen CD, et al. RNA-sequencing quantification of hepatic ontogeny of phase-I enzymes in mice. *Drug Metab Dispos* 2013;41:2175–86.

39. Peng L, Yoo B, Gunewardena SS, Lu H, Klaassen CD, Zhong XB. RNA sequencing reveals dynamic changes of mRNA abundance of cytochromes P450 and their alternative transcripts during mouse liver development. *Drug Metab Dispos* 2012;**40**:1198–209.
40. Cohen SM, Ellwein LB. Cell proliferation in carcinogenesis. *Science* 1990;**249**:1007–11.
41. Cohen SM, Ellwein LB. Genetic errors, cell proliferation, and carcinogenesis. *Cancer Res* 1991;**51**:6493–505.
42. Bieler CA, Stiborova M, Wiessler M, Cosyns JP, van Ypersele de Strihou C, Schmeiser HH. ³²P-post-labelling analysis of DNA adducts formed by aristolochic acid in tissues from patients with Chinese herbs nephropathy. *Carcinogenesis* 1997;**18**:1063–7.
43. Kohara A, Suzuki T, Honma M, Ohwada T, Hayashi M. Mutagenicity of aristolochic acid in the lambda/lacZ transgenic mouse (Muta-Mouse). *Mutat Res* 2002;**515**:63–72.
44. Paini A, Scholz G, Marin-Kuan M, Schilter B, O'Brien J, van Bladeren PJ, et al. Quantitative comparison between *in vivo* DNA adduct formation from exposure to selected DNA-reactive carcinogens, natural background levels of DNA adduct formation and tumour incidence in rodent bioassays. *Mutagenesis* 2011;**26**:605–18.